Adam Gacek
Witold Pedrycz *Editors*

ECG Signal Processing, Classification and Interpretation

A Comprehensive Framework of Computational Intelligence

Springer

ECG Signal Processing, Classification and Interpretation

Adam Gacek • Witold Pedrycz
Editors

ECG Signal Processing, Classification and Interpretation

A Comprehensive Framework of Computational Intelligence

Springer

Editors
Adam Gacek
Institute of Medical Technology
and Equipment
Roosevelta 118
41-800 Zabrze
Poland
adam.gacek@itam.zabrze.pl

Witold Pedrycz
Department of Electrical and Computer
Engineering
University of Alberta
116 Street 9107
T6G 2V4 Edmonton Alberta
Canada
pedrycz@ece.ualberta.ca

ISBN 978-0-85729-867-6 e-ISBN 978-0-85729-868-3
DOI 10.1007/978-0-85729-868-3
Springer London Dordrecht Heidelberg New York

British Library Cataloguing in Publication Data
A catalogue record for this book is available from the British Library

Library of Congress Control Number: 2011938277

Printed on acid-free paper

Springer is part of Springer Science+Business Media (www.springer.com)

Preface

ECG signals are one among the most important sources of diagnostic information. There has been a great deal of progress in the area of signal processing, classification, and interpretation in terms of the underlying signal acquisition technology itself as well as a variety of algorithmic and system developments supported by advanced information technologies. In the past decades, Computational Intelligence (CI) has emerged as a highly synergistic, computationally appealing, and conceptually unified framework supporting intelligent system design and analysis. Computational Intelligence promotes synergy. The key contributing technologies of CI – neurocomputing, fuzzy sets (or information granules and Granular Computing, in general), as well as evolutionary and population-based optimization – exhibit well-focused yet highly complementary research agenda. Neural networks are about learning and constructing nonlinear mappings. Fuzzy sets are concerned with the representation and organization of domain knowledge in terms of information granules – semantically meaningful entities, which are perceived and processed when describing and classifying real-world phenomena. Evolutionary computing is about forming a comprehensive optimization framework where structure and parameters of the system under design can be effectively developed.

From the perspective of ECG signal processing, classification, interpretation, and integration, the settings of Computational Intelligence bring forward a number of conceptually and computationally appealing and unique opportunities. The nonlinear nature of signal processing is well captured through neural networks. Information granules and their processing is essential to offer a significant level of interpretability of automatic classification systems. Information granules helps acquiring domain knowledge existing in the area. Evolutionary optimization becomes critical in supporting a structural development of classifiers.

As we are witnessing vigorous pursuits along this line of research and applied developments, we are also becoming aware of a very scattered nature of the material encountered in the literature. It becomes evident that there is a genuine need for a volume, which could offer a comprehensive, fully updated, and systematic exposure to the subject matter, addressing concepts, methodology, algorithms, and

case studies/applications. This edited volume intends to fill the gap. Our ultimate objective is to provide the reader with an in-depth, comprehensive material on the conceptually appealing and practically sound technology of Computational Intelligence and its use in the realm of ECG signal analysis, synthesis, classification, and interpretation.

With this objective in mind, the volume strives to articulate several focal points. We offer a systematic exposure of the concepts, design methodology, and detailed algorithms. Likewise, we stress a self-contained nature of the volume to enhance the exposure and readability of the material. We provide the reader with all necessary prerequisites and, if necessary, augment some parts with a step-by-step explanation of more advanced concepts supported by a significant amount of illustrative numeric material and some application scenarios to motivate the reader and make some abstract concepts more tangible. In particular, we offer a concise yet in-depth and well-focused exposure to Computational Intelligence as well as ECG signals themselves. The medical perspective at the ECG diagnostic content is offered as well. The systematic, well-organized flow of the presentation of the ideas is directly supported by a way in which the material is structured (with details presented in the next section of this book proposal). In general, we adhere to the top-down strategy by starting with the concepts and their underlying motivation and then proceeding with the detailed design that materializes in specific algorithms and representative applications and case studies. The individual chapters come with a clearly delineated agenda and a well-defined focus.

In what follows, we briefly highlight the main features of the chapters.

The opening chapter ***An Introduction to ECG Interpretation*** authored by J. Wasilewski and L. Poloński brings an important generic medical material. It offers an essential perspective at ECG signals regarded as an important source of vital diagnostic information and a way of its usage by medical specialists.

The chapter entitled ***An Introduction to ECG Signal Processing and Analysis*** by A. Gacek provides a comprehensive overview of the history, developments, and information supporting technology that is efficient and effective methods of processing and analysis of ECG signals with their emphasis on the discovery of essential and novel diagnostic information.

ECG Signal Analysis, Classification, and Interpretation: A Framework of Computational Intelligence authored by A. Gacek and W. Pedrycz is a general introduction to the principles, algorithms, and practice of Computational Intelligence (CI) and elaborates on those facets in relation with the ECG signal analysis. It discusses the main technologies of Computational Intelligence (neural networks, fuzzy sets, and evolutionary and population-based optimization), identifies their focal points, and stresses an overall synergistic character of the discipline, which ultimately gives rise to the highly synergistic CI environment. Furthermore, the main advantages and limitations of the CI technologies are discussed. The design of information granules is elaborated on; their design realized on the basis of numeric data as well as pieces of domain knowledge is considered.

The next chapter, ***A Generic and Patient-Specific Electrocardiogram Signal Classification System*** is authored by T. Ince, S. Kiranyaz, and M. Gabbouj. They report on a generic and patient-specific classification system designed for robust and accurate detection of ECG heartbeat patterns. They exploit the concept of morphological wavelet transform. By invoking its time–frequency localization properties inherent to wavelets, it becomes possible to separate the relevant ECG waveform morphology descriptors from the noise, interference, baseline drift, and amplitude variation of the original signal. The essential technologies of CI explored in this study stress an interesting synergy of neurocomputing where a neural network has been designed with the use of Particle Swarm Optimization (PSO).

P. Carvalho, J. Henriques, R. Couceiro, M. Harris, M. Antunes, and J. Habetha in their contribution entitled ***Model-Based Atrial Fibrillation Detection*** elaborate on the strategy based on a Computational Intelligence approach, combining expert knowledge and neural networks. This makes use of the three principal physiological characteristics being applied by cardiologists in their medical reasoning. Such a knowledge-based approach has an inherent advantage of increasing interpretability of the results, while improving robustness of the detection process. The authors exploit public databases (MIT-BIH Arrhythmia and QT databases from Physionet).

The principles and applicability of Evolutionary Computation (EC) are covered in the chapter entitled ***An Introduction to the Use of Evolutionary Computation Techniques for Dealing with ECG Signals*** and authored by G. Leguizamon and C.A. Coello. They present a comprehensive and carefully structured introduction to the EC fundamentals including a unified perspective of the most representative algorithms present in the area. Some other well-known bio-inspired metaheuristics that have been adopted for dealing with the treatment of ECG signals are also covered.

Diagnostic processes are knowledge-rich and knowledge-driven pursuits. To emphasize and exploit this aspect, M.H. Wang, C.S. Lee, G. Acampora, and V. Loia in their study entitled ***Electrocardiogram Application Based on Heart Rate Variability Ontology and Fuzzy Markup Language*** present a fuzzy markup language (FML)-based HRV ontology applied to the ECG domain knowledge. The ontology technologies are used to construct the personalized HRV ontology, and the FML is used to describe the knowledge base and rule base of the HRV. An experimental platform has been constructed to test the performance of the ontology.

The chapter entitled ***Learning in Artificial Neural Networks*** authored by A. Pâdua Braga offers a general overview of Artificial Neural Networks learning from the perspectives of Statistical Learning Theory and multi-objective optimization. The vital issue of a sound trade-off between the empirical risk obtained from the data set and the model complexity is elaborated on with direct implications on multi-objective learning. Subsequently, the main concepts of multi-objective learning are discussed in the context of ECG classification problems.

Kernel methods have recently enjoyed visible importance. The paper entitled ***A Review of Kernel Methods in ECG Signal Classification*** (J.L. Rojo Álvarez, G. Camps-Valls, A.J. Caamaño-Fernández, and J.F. Guerrero-Martínez) forms a well-rounded view at this recent technology by underlining their consistent and

well-founded theoretical framework for developing nonlinear algorithms. It is shown that kernel characteristics are particularly appropriate for biomedical signal processing and analysis, and hence one can witness the widespread use of these techniques in biomedical signal processing in general, and in ECG data analysis, in particular. This chapter provides a survey of applications of kernel methods in this context of ECG signal analysis.

G. Bortolan, I. Christov, and W. Pedrycz in the chapter, ***Hyperellipsoidal Classifier for Beat Classification in ECG Signals,*** stress important interpretability facets of ECG pattern classifiers by presenting so-called hyperbox classifiers. Different techniques based on a combination of fuzzy clustering and genetic algorithms are put together to form an efficient learning environment. The hyperbox classifiers have been investigated for the detection and classification of different types of heartbeats in electrocardiograms (ECGs), which are of major importance in the diagnosis of cardiac dysfunctions. The experiments were reported for the MIT-BIH arrhythmia database. The chapter elaborates on several ways of combining fuzzy clustering and genetic algorithm in identifying the optimal hyperboxes and forming a family of hyperellipsoids.

A.I. Hernandez, J. Dumont, M. Altuve, A. Beuchee, and G. Carrault in their study, ***Evolutionary Optimization of ECG Feature Extraction Methods: Applications to the Monitoring of Adult Myocardial Ischemia and Neonatal Apnea Bradycardia Events,*** propose an automated method, based on evolutionary computing, to optimize parameters used in signal processing methods (filter cut-off frequencies, thresholds, etc.) being applied to ECG signals. This is of particular importance for signal processing applied to the detection and segmentation of individual ECG beats. This optimization method is described and applied to two different monitoring applications, namely the detection of myocardial ischemia episodes on adult patients and the characterization of apnea-bradycardia events in preterm infants.

Given the organization of the material, the volume could serve as a useful reference material for graduate students and senior undergraduate students in courses in biomedical system design expert systems, bioinformatics, and bioengineering, especially those aimed at ECG signal analysis and interpretation. The volume will appeal to the practitioners. The book brings forward a new conceptual and algorithmic framework of Computational Intelligence to the practice of biomedical signal processing.

We would like to take this opportunity to express our sincere thanks to the authors for reporting on their innovative research and sharing insights into the area. The reviewers deserve our thanks for their constructive input. We highly appreciate a continuous support and professionalism of the staff of Springer.

We hope that the readers will find this publication of genuine interest and help in research, educational, and practical endeavors.

Zabrze, Poland — *Adam Gacek*
Edmonton, Alberta, Canada — *Witold Pedrycz*

Contents

Chapter 1
An Introduction to ECG Interpretation

Jarosław Wasilewski and Lech Poloński

1.1 Introduction

Electrocardiography is a method that registers electrical activity against time. The changes in electrical potential difference (voltage) during depolarization and repolarisation of the myocardial fibers are recorded by electrodes positioned on the surface of the chest and on the limb (limb leads). The sources of the electrical potentials are contractile cardiac muscle cells (cardiomyocytes). The ECG waveform is either printed onto graph paper that runs at a constant speed or shown on a computer screen. The advantages of electrocardiography come with its low cost, immediate availability and easy implementation. The procedure itself is also non-invasive.

The electrocardiogram (ECG) is used to investigate some types of abnormal heart function including arrhythmias and conduction disturbances, as well as heart morphology (e.g., the orientation of the heart in the chest cavity, hypertrophy, and evolving myocardial ischemia or infarction). It is also useful for assessing performance of pacemarkers.

1.2 The Electrical Conduction System of the Heart

Cardiac muscle is composed of two main cell types: cardiomyocytes, which generate electrical potentials during contraction, and cells specialized in the generation and conduction of the action potentials. These specialized electrical cells depolarize spontaneously. At rest, cardiomyocytes are polarized with an electrical membrane

J. Wasilewski (✉) · L. Poloński
Silesian Center for Heart Disease, Zabrze ul. Marii Skłowowskiej-Curie 9, Zabrze, Poland
e-mail: jarosław-wasilewski@wp.pl; scchs@slam.katowice.pl

A. Gacek and W. Pedrycz (eds.), *ECG Signal Processing, Classification and Interpretation: A Comprehensive Framework of Computational Intelligence*,
DOI 10.1007/978-0-85729-868-3_1, © Springer-Verlag London Limited 2012

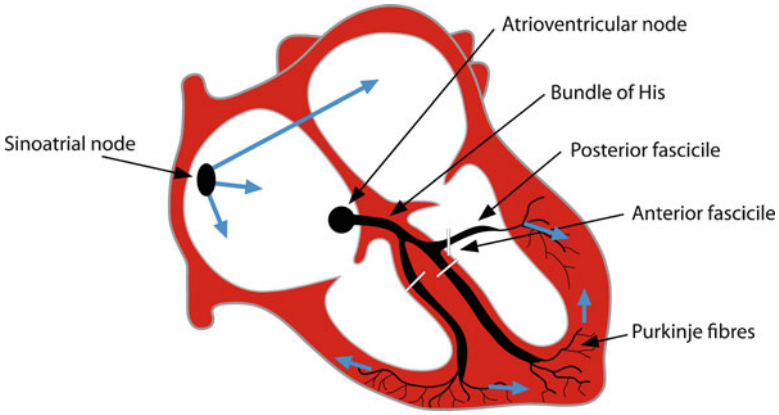

Fig. 1.1 The electrical conduction system of the heart

potential of about −90 mV. Excitation by an external stimulus can trigger a rapid reversal of the electrical potential of working myocardial cells (depolarization). The depolarization is usually due to a sudden increase in permeability of the membrane to sodium, which allows positively charged sodium ions to enter the cell. In some cardiac cells the action potential is carried by calcium ions instead of sodium ions. The downward swing of the action potential, or repolarisation phase, is mainly due to the movement of potassium ions out of the cell. After depolarization, the muscle returns to its original electrical state. During the repolarisation, the cardiac muscle is incapable of being stimulated (i.e., is refractory), which protects it against premature activation.

The conduction system of the heart is shown in Fig. 1.1. The sinoatrial node (S-A) has the highest rate of spontaneous depolarization and acts as the primary pacemaker. At normal condition, the S-A node generates impulses that stimulate the atria to contract. This node is located in the superior wall of the right atrium, close to the opening of the superior vena cava. Other elements of the conduction system include the atrioventricular node (A-V), located between the atria and the ventricles, in the lower atrial septum adjacent to the annulus of the mitral valve, and the bundle of His. The bundle of His divides into a right and left branch at the level of membranous part of the interventricular septum. The left branch is further branched into an anterior and posterior bundle. The Purkinje fibers are the final component of the conduction system, which are intertwined with muscle fibers and the papillary muscles. Their task is to conduct the wavefronts directly to the two ventricles so that they contract simultaneously. The Purkinje fibers have intrinsic automaticity (ventricular escape rhythm) generating approximately 30 bpm (beats per minute). The cells of the A-V node also depolarize spontaneously but at a higher rate (about 40–50 bpm) and this automaticity is called (escape) junctional rhythm. In physiological conditions the automaticity of these rescue pacemakers is suppressed by the activity of the S-A node.

If electrical activity appears on the ECG recording later than expected (i.e., the R-R interval is longer than the R-R interval in sinus rhythm), this means that an action potential originated in one of the lower pacemakers. However, the appearance of activity earlier than expected indicates the presence of a premature ectopic beat.

Extrasystolic beats are usually followed by compensatory pause. A full compensatory pause occurs after ventricular premature beats, see Fig. 1.16, and an incomplete compensatory pause occurs in cases of supraventricular premature beats. This happens because of the depolarization of the A-V node if the activity is supraventricular and its changes firing rate of the S-A node (Fig. 1.4).

The activity of the S-A node is regulated mainly by the autonomic nervous system. An activation of sympathetic fibers causes an increase in the heart rate, while activation of the parasympathetic fibers results in a decrease in this rate. The normal heart rate at rest is approximately 60–70 bpm but is lower at night during sleep. The heart rhythm is normally regular except for minor variations with respiration especially in young individuals.

Using the terminology associated with electrical devices, the conduction system of the heart can be described as a pacemaker (S-A node), a resistor that simultaneously acts like a fuse (the A-V node) and two insulated electrical cables (branches of the bundle of His) (Fig. 1.1). The term "resistor" for the property of the A-V node is appropriate because it slows down the depolarization (conduction velocity through the A-V node is slower than in other parts of the conducting system −0.05 m/s vs. 4 m/s, respectively). This delay enables the transfer of blood from the atria to the ventricles and is responsible for ensuring that the sequence of ventricular contraction follows atrial contraction.

The comparison between the A-V node and a "fuse" is appropriate because the A-V node possesses Wenckebach's point, which is thought to maintain the ratio of maximum conduction of the supraventricular impulses to ventricles at 1:1. Under normal conditions this is about 180 impulses/min. In certain situations, such as in atrial fibrillation, Wenckebach's point provides protection against the propagation of atrial fibrillation to ventricular fibrillation. In the presence of accessory conduction pathways bypassing the atrioventricular A-V node, this mechanism can fail and atrial flutter or fibrillation can therefore progress to ventricular flutter or fibrillation.

A properly functioning conduction system guarantees an appropriate heart rate and sequential contractions of the atria and ventricles. Cardiac electrical dysfunction can be caused by damage to or improper functioning of any of the components of the conduction system separately or in combination with other problems (for example, sinus bradycardia and bundle-branch block). Other causes of cardiac arrhythmias can be a pathological stimulus generation (for example, premature ectopic beats) or pathological conductive loops. Re-entry, which is a recurrence of electrical impulses, is the most common mechanism responsible for the occurrence of paroxysmal and persistent tachycardia. A common arrhythmia that arises in this manner is atrial flutter. For this phenomenon to occur, a re-entry circuit formed by two conduction pathways is necessary. Impulses in the first pathway travel at ahigh velocity (the fast pathway) while impulses in the second pathway travel at a

considerably lower velocity (the slow pathway). This means there is a delay between the arrival of the two signals, so that when the second impulse arrives, the cells are no longer refractory.

1.3 Electrical Axis and Orientation of the Heart in the Chest Cavity

Bipolar limb leads (I, II, III) developed by Willem Einthoven (Fig. 1.2) aim to calculate the mean depolarization vector of the heart in the frontal plane (the electrical axis of the heart) (Figs. 1.20a, b). The normal range of the electric axis lies between $+30^\circ$ and -110° in the frontal plane.

The morphology of the ECG recorded depends on the orientation of the heart. The unipolar augmented limb leads of Goldberger (aVR, aVL, and aVF) are used in determining the orientation of the heart. If the position of the heart is vertical as, for example, in asthenic women, the net deflection of the QRS complex in lead aVF is positive and it resembles lead V6 in morphology. Meanwhile, the QRS complex

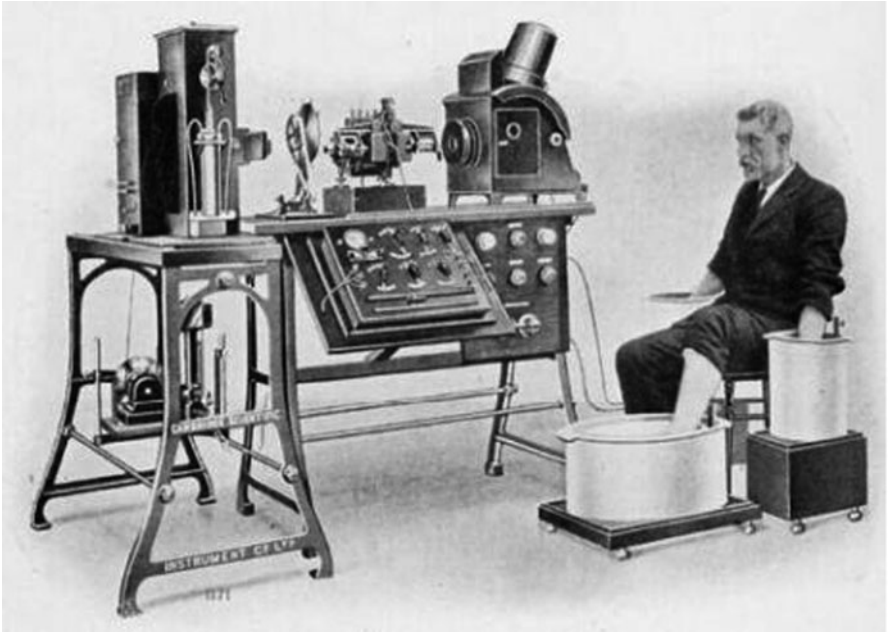

Fig. 1.2 The ECG machine constructed by Willem Eindhoven (1860–1927). The patient is connected to the galvanometer and both hands and one leg are immersed in saline containers. The electrodes connected by cables to the galvanometer are called the limb leads. Eithoven was awarded the Nobel Prize for his discovery of mechanism of electrocardiography

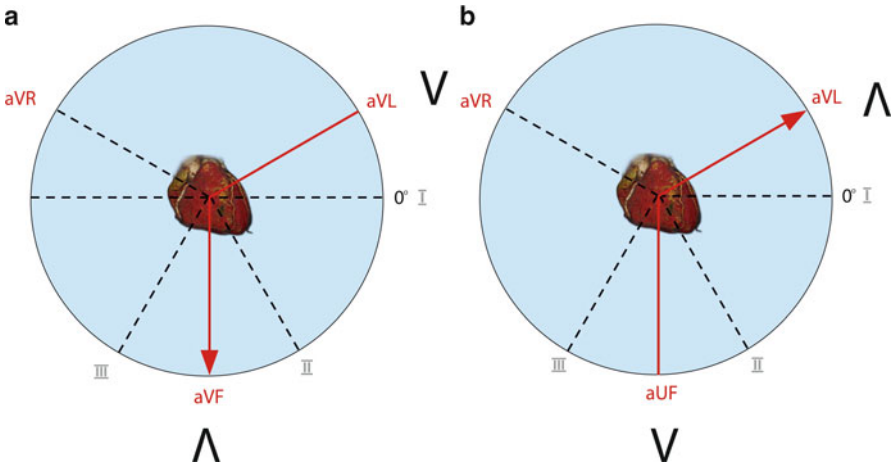

Fig. 1.3 The orientation of the heart in chest cavity. *Panel* (**a**) – vertical position. *Panel* (**b**) – horizontal position of the heart. A fundamental principle of ECG recording is that when the wave of depolarization travels toward a recording lead this results in positive or upward deflection. In contrast, if the wave of depolarization travels away, it results in negative or downward deflection

in lead aVL is negative and resembles lead V1 (Fig. 1.3a). In contrast, when the orientation of the heart is horizontal, for example, in an endomorphic individual or in someone whose diaphragm is in a high position, the QRS complex in lead aVF resembles lead V1 (the net deflection of the QRS complex is negative) and lead aVL resembles lead V6 (Fig. 1.3b).

The placement of Wilson's unipolar precordial leads is as follows:

V1: 4th intercostal space, right of the sternum
V2: 4th intercostal space, left of the sternum
V3: halfway between V2 and V4
V4: 5th intercostal space, left midclavicular line
V5: anterior axillary line, where it is intersected by a perpendicular line from lead V4
V6: midaxillary line, where it is intersected by a perpendicular line from lead V4

The chest leads sense the ECG in the transverse or horizontal plane. Leads V1 and V2 are placed above the anterior wall of the right ventricle. For this reason they are referred to as right ventricular leads. When the heart is normally oriented along the long axis, leads V5 and V6 are placed above the lateral wall of the left ventricle and are therefore known as left ventricular leads. The transitional zone between the left and right ventricles (interventricular septum) is found at the level of lead V3 and V4 (equal amplitudes of the R-wave and S-wave). In cases where the heart is rotated around its long axis the transitional zone is displaced, for example during an acute pulmonary embolism. The right ventricle is enlarged in this situation and the transitional zone is often shifted to the right toward the leads V5 or even V6

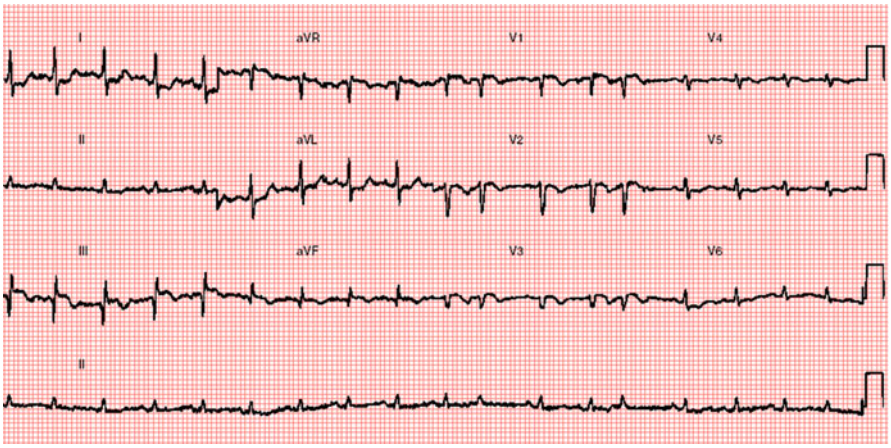

Fig. 1.4 Acute pulmonary embolism. The transitional zone in the chest leads is located near lead V5. In this situation the right ventricular leads are V1–V4. The first left ventricular lead is V6. This ECG shows the ST segment elevation in leads III, aVF, and V1–V3 with negative T-waves in these leads (characteristic pattern of ischaemia of the right ventricle). The eleventh and fourteenth cardiac cycles are premature supraventricular beats. The compensatory pause is incomplete. The RR interval including premature contractions is shorter than double the regular R-R interval of sinus rhythm (This figure was published in Poloński and Wasilewski (2004), p. 8, Fig. 2.4. Copyright Elsevier Urban & Partner Sp. z.o.o, 2006, Wrocław)

(see Fig. 1.4). According to the ECG shown in Fig. 1.4 the right ventricular leads are V1–V4 and the left ventricular lead is V6. For this reason, the right ventricular leads are best defined as lying to the right of the transitional zone, while the left ventricular leads lie to the left of the transitional zone. In patients with cyanotic congenital heart defect with significant hypertrophy and enlargement of the right ventricle, most or even all of the precordial leads can be found overlying the right ventricle. In these situations the displacement of the transitional area is accompanied by a high voltage wave in V1 and V2, which is typical for right ventricular hypertrophy.

1.4 Waves, Segments, and Intervals

There are certain elements in the ECG waveform (Fig. 1.5):

- The isoelectric line: a horizontal line when there is no electrical activity on ECG.
- Segments: the duration of the isoelectric line between waves
- Intervals: the time between the same segments of adjacent waves.

The P-wave is the first deflection of the ECG. It results from depolarization of the atria. Atrial repolarisation occurs during ventricular depolarization and is obscured. The QRS complex corresponds to the ventricular depolarization.

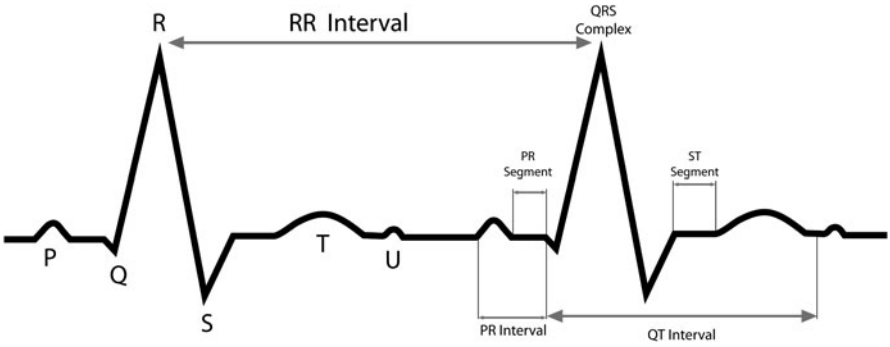

Fig. 1.5 The ECG waves, segments, and intervals

The T-wave represents ventricular repolarisation, i.e., restoration of the resting membrane potential. In about one-quarter of population, a U-wave can be seen after the T-wave. This usually has the same polarity as the preceding T-wave. It has been suggested that the U-wave is caused by after-potentials that are probably generated by mechanical–electric feedback. Inverted U-waves can appear in the presence of left ventricular hypertrophy or ischaemia.

The PQ segment corresponds to electrical impulses transmitted through the S-A node, bundle of His and its branches, and the Purkinje fibers and is usually isoelectric. The PQ interval expresses the time elapsed from atrial depolarization to the onset of ventricular depolarization. The ST-T interval coincides with the slow and rapid repolarisation of ventricular muscle. The QT interval corresponds to the duration of the ventricular action potential and repolarisation. Then TP interval is the period for which the atria and ventricles are in diastole. The RR interval represents one cardiac cycle and is used to calculate the heart rate.

1.5 Interpretation of the ECG

After describing the predominant heart rhythm, the mean electrical axis, and the position of the heart in the chest, the next step of the ECG analysis is to evaluate the shape, amplitude, and duration of the waves, segments, and intervals.

1.6 The P-wave

The P-wave is usually positive in most leads (but it is always negative in aVR) (Fig. 1.18). It can sometimes have a negative deflection in leads III and V1 or be biphasic in these leads and in lead aVL. The normal duration of the P-wave is

no longer than 0.12 s, and the voltage in the limb leads should not exceed 0.25 and 0.15 mV in the precordial leads. A P-wave that is notched, and exceeds the values given above (voltage, duration, and polarization in the appropriate leads) is considered abnormal. This can result from atria enlargement and hypertrophy or from atrial depolarization generated in locations other than the S-A node.

1.7 The PQ Interval

The normal range for the PQ interval is 0.12–0.20 s. Longer PQ intervals are seen in cases of first- or second-degree atrioventricular block. The PQ interval can be shortened in pre-excitation syndromes, in which depolarizations from the atria are transmitted to the ventricles via an anomalous accessory conduction pathway that bypasses the A-V node.

1.8 The QRS Complex

This is the largest group of waves on the ECG and represents ventricular depolarization. The first downward deflection is the Q-wave. The first upward deflection is called the R-wave. The S-wave is the last downward deflection of the QRS complex. The Q-wave is not a constant component of the QRS (ventricular) complex.

During physiological conduction through the branches of the bundle of His, the left and right ventricle are depolarized simultaneously and contract along the direction of ventricular outflow tract. Ventricular depolarization propagates from the medial part of the septum downward through the apex of the heart and further along the free wall of the ventricles toward the base of the heart. The normal duration of the QRS complex does not exceed 0.12 s. The voltage usually varies between 1.5 and 2.0 mV. Durations greater than 0.12 s are most likely due to an asynchronous depolarization of both ventricles. This occurs in cases of bundle-branch block, pre-excitation syndromes, or premature ventricular contraction. In these situations, one ventricle is depolarized earlier than the other. In such cases the QRS complex consists of one R-wave followed by an R'-wave. These waves correspond to the depolarization of one and then the other ventricle, respectively. In this situation the QRS complex gets subsequently wider. If the widened and notched QRS complex is most pronounced in the right ventricular leads V1 and V2 (Fig. 1.6) then it could be caused by a right bundle-branch block. Analogously, if a notched QRS complex is recorded in the left ventricular leads V5 and V6, it may result from a left bundle-branch block (Fig. 1.7). If there is a pre-excitation syndrome with an accessory conduction pathway located on the right side, then the QRS complex mimics left bundle-branch block morphology. Similarly, if a premature beat originates in the right ventricle, then the QRS complex can also resemble left bundle-branch block. In both of these situations the right ventricle is

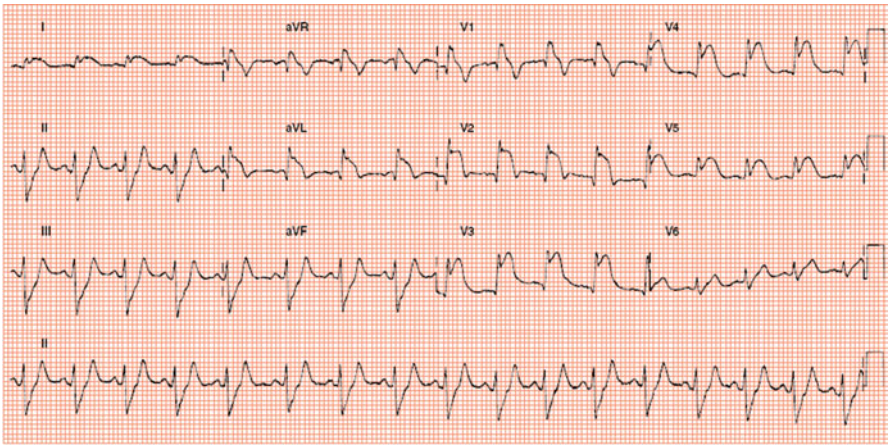

Fig. 1.6 Right bundle-branch block during an anterior wall MI showing ST segment elevation in leads V1–V6 and in leads I and aVL. There is a reciprocal ST segment depression in leads II, III, and aVF (This figure was published in Poloński and Wasilewski (2004), p. 112, Fig. 10.1.2a. Copyright Elsevier Urban & Partner Sp. z.o.o, 2006, Wrocław)

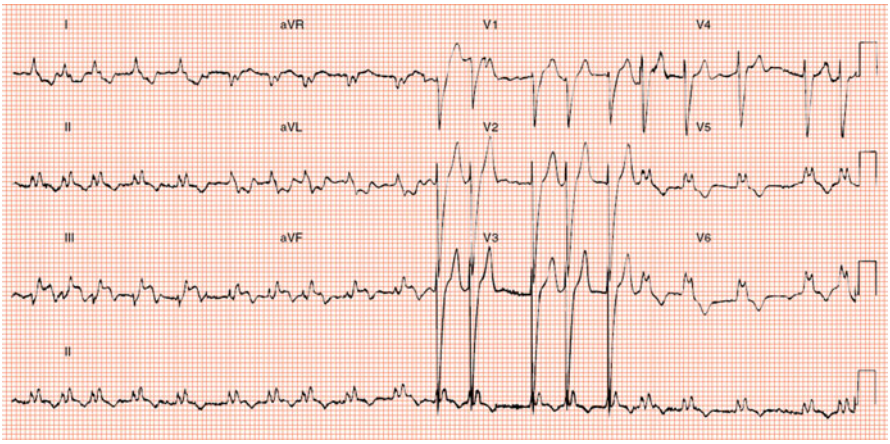

Fig. 1.7 Irregular heart rhythm (atrial fibrillation and left bundle-branch block). Notched and widened QRS complex with secondary changes in the ST segment and T-wave (ST segment depression and T-waves opposite to net deflection of QRS complex). Note the ST segment elevation in leads II, II and aVF (an inferior wall MI) (This figure was published in Poloński and Wasilewski (2004), p. 118, Fig. 10.2.2. Copyright Elsevier Urban & Partner Sp. z.o.o, 2006, Wrocław)

depolarized first, as in left bundle-branch block. In pre-excitation syndromes with an accessory conduction pathway located on the left side of the heart, or when a premature beat originates in the left ventricle, the widened QRS complex occurs in the right ventricular leads. In this case the QRS complex will resemble right

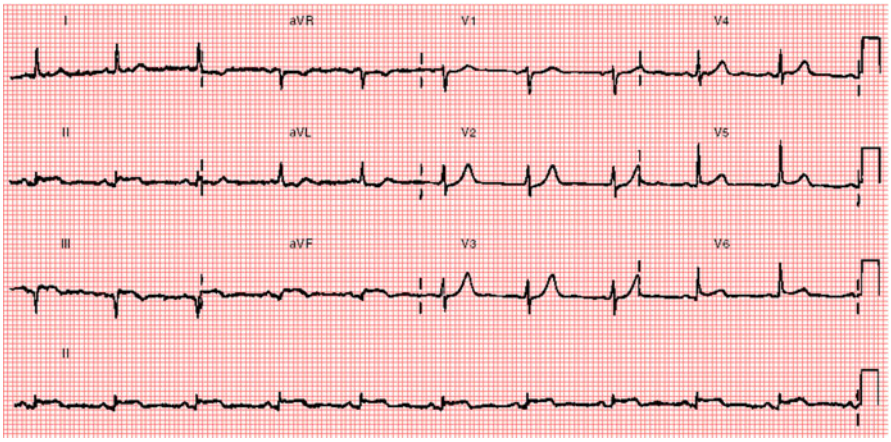

Fig. 1.8 ST segment elevation in lead III equal to the elevation in lead II, with a reciprocal ST segment depression in lead aVL. ST segment in lead I runs in the isoelectric line. The QS complex is present in leads III and aVF. ST segment elevation in leads V5 and V6. High R-wave (R-wave voltage is greater than S) in lead V2 with a positive T-wave. Evolution of inferoposterolateral wall MI (This figure was published in Poloński and Wasilewski (2004), p. 81, Fig. 8.1.5. Copyright Elsevier Urban & Partner Sp. z.o.o, 2006, Wrocław)

bundle-branch block (Fig. 1.16). Widening of the QRS complex is also seen in ventricular hypertrophy although in this situation the voltage criteria for hypertrophy must also be satisfied.

A small Q-wave is present in leads V5 and V6 and comes as a manifestation of depolarization of the septum. Each Q-wave in the precordial leads (except for the QS complex in V1) or widened and deep Q-waves in leads V5 or V6 are considered to be pathological and indicate the presence of necrotic tissue after a myocardial infarction (MI). A Q-wave in leads II, III, and aVF is considered pathological when the duration is longer than 0.03 s and its amplitude greater than 25% of the height of the R-wave and 50% of the voltage of the R-wave in lead aVL. In the case of a myocardial scar of the left ventricle posterior wall the equivalent of a Q-wave in leads V1 and V2 is an R-wave greater than the S-wave in one of these leads. Usually in this situation, the T-wave in leads V1 and V2 is positive (Figs. 1.8 and 1.16).

1.9 The ST Segment

The ST segment is a part of the ECG from the QRS complex (the J point) to the onset of the T-wave. It is normally isoelectric. The most important reason for ST segment elevation is an MI (Fig. 1.9), but it can also occur in the course of other diseases such as pericarditis (Fig. 1.10) and pulmonary embolism (Fig. 1.4) or can be a persistent abnormality in subjects with a post-MI left ventricular aneurysm.

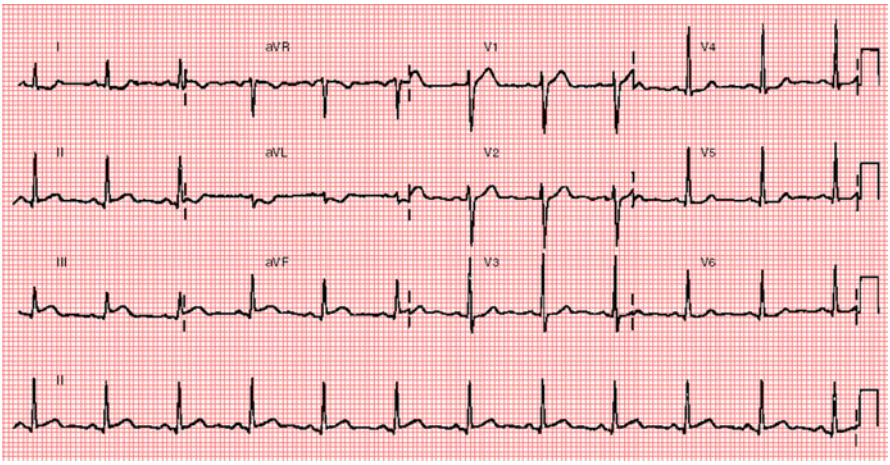

Fig. 1.9 ST segment elevation in leads II, III, and aVF. The ST segment elevation in lead III is higher than in lead II. The ST segment elevation in the right ventricular lead V1 and the lack of a reciprocal ST segment depression in lead V2 indicate that the MI of the inferior wall of the left ventricle is accompanied by a right ventricular MI (This ECG pattern suggests right coronary occlusion above the origin of the right ventricular branch) (This figure was published in Poloński and Wasilewski (2004), p. 94, Fig. 8.2.5a. Copyright Elsevier Urban & Partner Sp. z.o.o, 2006, Wrocław)

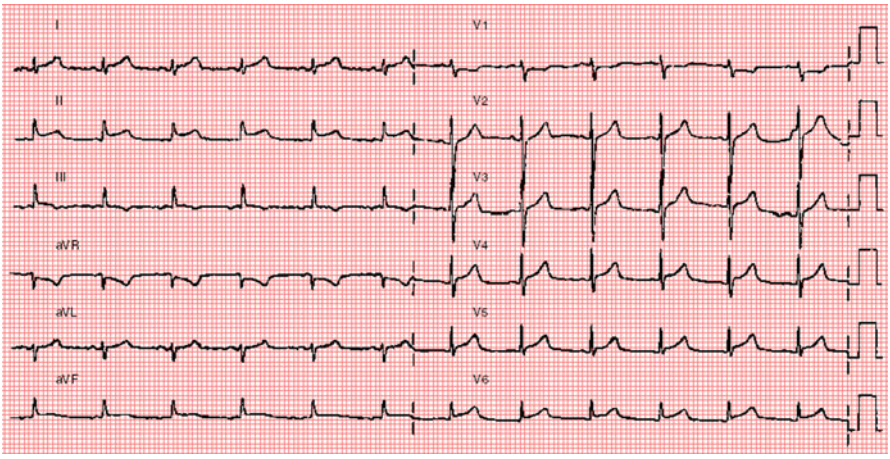

Fig. 1.10 Acute pericarditis. The widespired ST segment elevation. ST segment depression in leads aVR and V1. Note the upward concavity of the ST segment elevation and notching at the J point in leads I, II, III, and V4–V6 (This figure was published in Poloński and Wasilewski (2004), p. 6, Fig. 2.1. Copyright Elsevier Urban & Partner Sp. z.o.o, 2006, Wrocław)

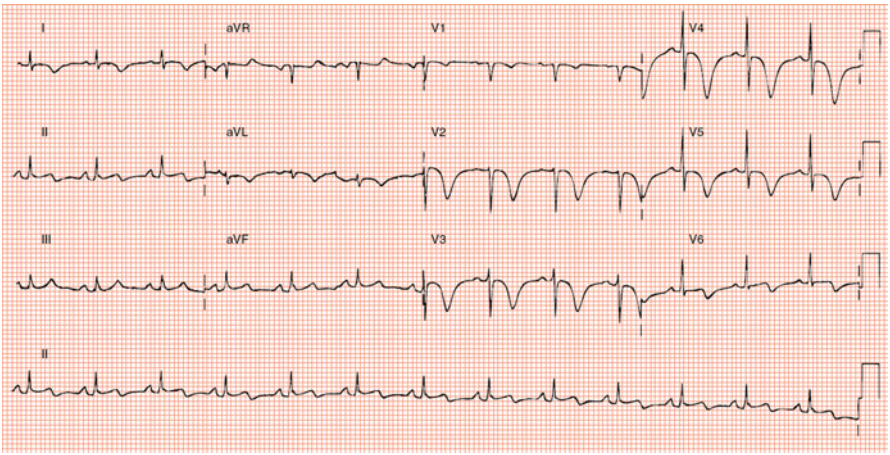

Fig. 1.11 Anterior wall MI during an occlusion of the anterior descending artery (LADT-wave pattern). Note the presence of deep symmetrical negative T-waves in leads V2–V5 and negative T-wave in leads I and aVL, biphasic T-wave in lead V6 and a positive T-wave in lead aVR (This figure was published in Poloński and Wasilewski (2004), p. 11, Fig. 2.6a. Copyright Elsevier Urban & Partner Sp. z.o.o, 2006, Wrocław)

Other situations include a dissecting aortic aneurysm (if the dissection involves the ostium of the coronary arteries), Brugada's syndrome, hyperkalaemia, hypothermia, hypervagotonia, and early repolarisation syndrome. A displacement of the ST segment secondary to the alternation of the sequence of depolarization accompanies bundle-branch block (Figs. 1.7 and 1.16), prexcitation syndromes, and premature ventricular contraction (T-wave polarity opposite to that of the R wave).

An ST segment depression in leads aVR and V6 with an ST elevation in most of the leads is found in exudative pericarditis (Fig. 1.10). A horizontal or oblique downward depression, of the ST segment, especially in patients with chest pain, is the most specific sign of ongoing myocardial ischaemia.

1.10 T-Wave

The T-wave should be positive in most leads except for aVR and sometimes in V1, in which it can be horizontal or negative. Deeply negative T-waves can be a sign of MI, e.g., due to occlusion of the left anterior descending artery (LAD-T-wave pattern) (Fig. 1.11). Other situations include hypertrophic cardiomyopathy and subarachnoid haemorrhage. T-wave inversion sometimes occurs without obvious causes (idiopathic global T-wave inversion).

1.11 The QT Interval

The QT interval is measured from the beginning of the QRS complex to the end of the T-wave. The length of the QT interval is directly affected by the heart rate (the slower the heart rate, the longer the interval). To eliminate this influence, a corrected QT (QTc) should be calculated using either Bazett's formula ($QTc = QT/RR^{0.5}$) or Fridericia's formula ($QTc = QT/RR^{0.33}$). The disadvantage is that these formulas overestimate the QT interval when the heart rate is fast and underestimate it when the heart rate is slow. Prolongation of the QT interval can be caused by many factors, including some medications, and it is also associated with the increased risk of polymorphic tachycardia known as torsades des pointes ("twisting of the points") – sudden cardiac death can result (Dessertenne 1966). The normal range for the QT interval is up to 0.44 s.

1.12 Adjacent and Opposing Leads

When assessing the ECG it is important to be familiar with the adjacent and opposing leads. The placement of the leads in relation to the structure of the heart is shown in Fig. 1.12. The adjacent leads are: lead II and aVF and lead aVF and III. These leads represent the inferior wall of the left ventricle. The adjacent limb leads are also leads I and aVL, and represent the basal segment of the left ventricle. Among precordial leads adjacent leads are for example V5 and V6 placed in front of the lateral wall of the left ventricle. The opposing leads (groups of leads where the displacement of the ST segment in one direction is accompanied by the displacement of the ST segment in the reciprocal direction in the other group of leads) are defined as follows: leads I and aVL are opposing to leads II, III, and aVF; whether the highest ST segment elevation is seen in lead aVL, the deepest ST segment depression is present in lead III (Fig. 1.13). In unipolar leads opposing leads for V1 and V2 are leads V7 and V8 covering the posterior wall. In a plane perpendicular to the front of the limbs, the reciprocal ST segment depression in leads V1–V3 are present, with an ST elevation in the inferior wall leads or as an ST elevation in lead aVR with an ST segment depression in lead V6 and vice versa.

Knowledge about adjacent and opposing leads is necessary for assessing ECG changes seen in an ST elevation MI and helps determine the infarct-related artery, and even the localization of the occlusion. In case of an inferior wall infarct caused by occlusion of the right coronary artery, the displacement of the vector of the ST segment elevation in the limb leads is to the right, while in a myocardial infarction associated with occlusion of the circumflex coronary artery, the displacement of the ST segment elevation vector is to the left. The association between the ECG, the angiographic localization of the infarct, and diagnostic algorithms is discussed in further detail elsewhere (Poloński and Wasilewski 2004).

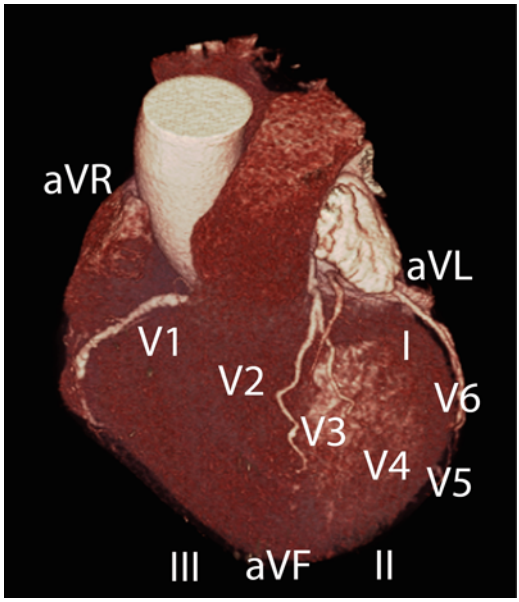

Fig. 1.12 Myocardial infarction due to the right coronary artery, the vector of the ST segment elevation is directed to the right toward lead III (the ST segment elevation in lead III is greater than in lead II and the ST segment depression in lead aVL is greater than in lead I). If the left circumflex artery is responsible for the MI then the ST segment elevation is in lead II $\geq$ III and there is no ST segment depression in lead I (the ST segment elevation vector is directed to the left toward lead II). In an anterior wall MI the highest ST segment elevation is seen in leads V2 and V3. In a MI with occlusion of the diagonal artery or the marginal artery, ST segment elevation appears in leads I and aVL, which are the leads representing the basal segment of the heart (Fig. 1.13). ST segment elevations are accompanied by ST segment depression in the opposite leads (reciprocal or reflected ST depression)

1.13 Negative or "Inverted" Leads

Negative leads are leads that are not present in the 12-lead ECG but are formed by inversion of the 12 standard leads. The angle between them, in contrast with the opposite leads, is always 180° (opposite orientation). The names of the negative leads are analogous to the 12 standard leads, but are preceded by a minus sign. An ECG in which negative leads are analyzed is called a 24-lead ECG. It offers supplemental clinical information without increasing the number or even altering the position of the 10 standard electrodes (Figs. 1.13 and 1.15).

Even though leads V1 (V2R) and V2 (V1R) are defined as right ventricular leads, this designation is not precise. In the absence of hypertrophy or enlargement of the right ventricle, these leads represent a view of the left ventricle posterior wall as a mirror image (Figs. 1.14–1.17). The action potential of the right ventricle is too small to have any vital influence on the ECG waveform in these leads. Consequently,

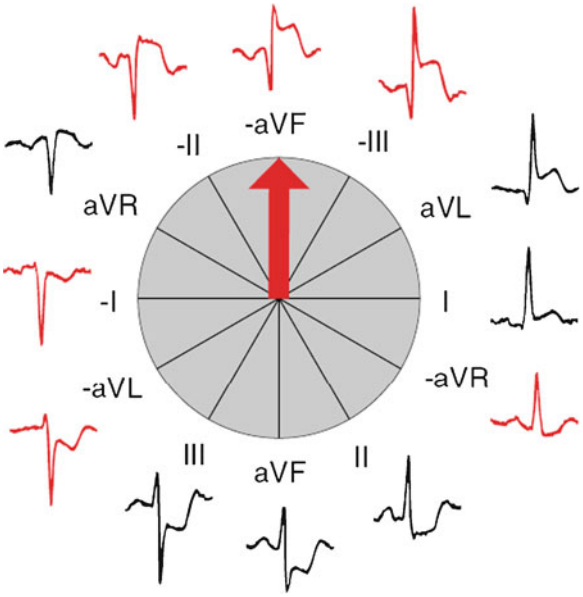

Fig. 1.13 The limb leads and corresponding negative limb leads. ST segment depressions in leads II, aVF, and III represent reciprocal ST segment elevation on the opposing leads I and aVL. Displacement of the ST segment is also seen in the all negative leads. MI of the basal segment of the heart due to occlusion of the diagonal branch (This figure was published in Poloński and Wasilewski (2004), p. 35, Fig. 2.1c. Copyright Elsevier Urban & Partner Sp. z.o.o, 2006, Wrocław)

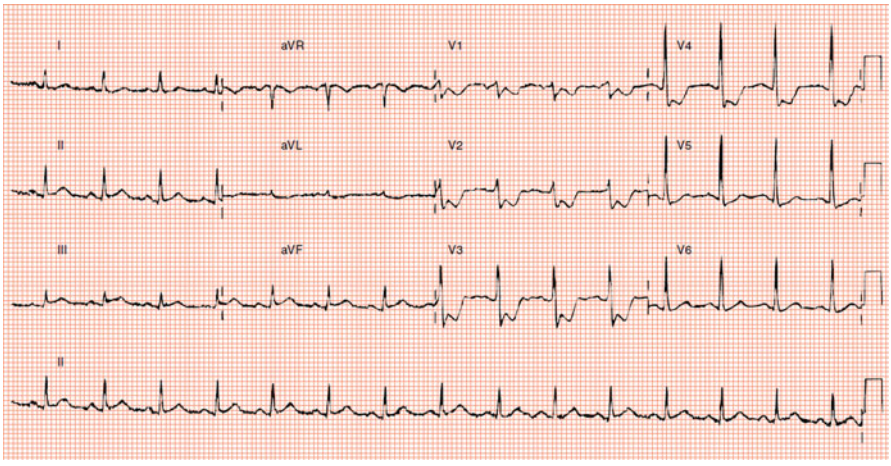

Fig. 1.14 ST segment elevation in leads II, III, and aVF, in which the elevation in lead II is equal to that in lead III. A small reciprocal ST segment depression can be seen in lead aVL. A reverted Pardee wave is present in leads V1–V4 ("up-sidedown injury"). ST segment elevation in lead V6. Inferoposterolateral wall MI. Diagnosis of posterior wall MI was made from reciprocal changes appear in leads V1–V4 (This figure was published in Poloński and Wasilewski (2004), p. 98, Fig. 8.4.3a. Copyright Elsevier Urban & Partner Sp. z.o.o, 2006, Wrocław)

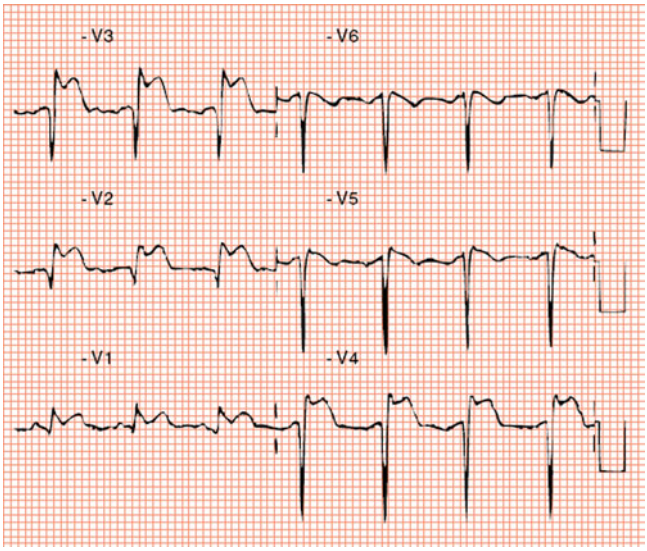

Fig. 1.15 Precordial leads shown in Fig. 1.14 are presented as their negative counterpart. Pardee's wave is clearly seen in leads −V1 to −V4. The maximal information that could be gained without the placement of additional electrodes but adding inverted leads for evaluation of ST-segment displacement (This figure was published in Poloński and Wasilewski (2004), p. 99, Fig. 8.4.3c. Copyright Elsevier Urban & Partner Sp. z.o.o, 2006, Wrocław)

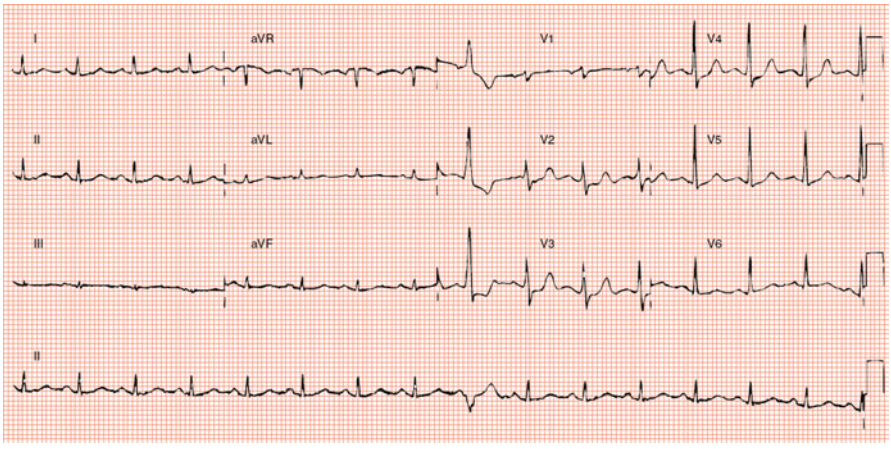

Fig. 1.16 The same patient as in Fig. 1.14, but the ECG is recorded 1 h after the patency of the artery has been restored. Note the high voltage R-wave in lead V2 (the amplitude of R-wave is greater than S) and a positive T-wave. The ninth cardiac cycle is a premature ventricular beat. The RR interval that contains the extrasystole is twice as long as the RR interval in sinus rhythm. A full compensatory pause is present. The premature ventricular contraction has morphology that resembles a right bundle-branch block and indicates that the premature ventricular contraction originates in the left ventricle (This figure was published in Poloński and Wasilewski (2004), p. 99, Fig. 8.4.3b. Copyright Elsevier Urban & Partner Sp. z.o.o, 2006, Wrocław)

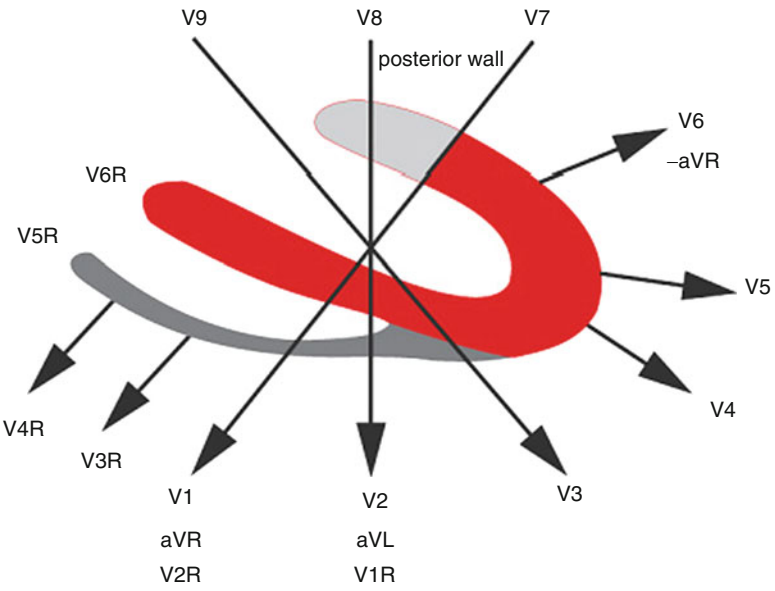

Fig. 1.17 The schematic diagram shows the placement of the precordial leads and their position in relation to leads aVL and aVR. The opposite leads related to leads V1 and V2 are leads V7 and V8 (This figure was published in Poloński and Wasilewski (2004), p. 29, Fig. 5.1. Copyright Elsevier Urban & Partner Sp. z.o.o, 2006, Wrocław)

the right ventricle is said to be "invisible" in the ECG. Under this assumption, the equivalent of the small Q-wave in V6 is a small R-wave in lead V1. The equivalence of a high R-wave in V6 is a deep negative S-wave in lead V1. The theory of opposite leads helps explain why, in case of left ventricular hypertrophy, there is an increase in the R-wave voltage in lead V6, which is accompanied by further S-wave voltage increase in lead V1. According to the Sokolow-Lyon index, left ventricular hypertrophy can be diagnosed when the sum of the voltages of the R-wave in V6 and the S-wave in V1 is greater than 35 mV (Sokolow and Lyon 1949).

Knowledge of adjacent and opposite leads not only helps to identify the orientation of the heart axis but also explains why, in lead aVR, the P-waves and T-waves and QRS complex are negative (Fig. 1.18). It also explains why in left axis deviation the QRS complex is positive in lead I and negative in lead III. If the average of depolarization vector in frontal plane is moving toward an electrode, this electrode records a positive deflection (lead I). At the same time, a wave of depolarization is moving away from lead III and this lead records a negative deflection (Figs. 1.19 and 1.20a). This effect is reversed if the electrical axis deviates to the right. Then the depolarization vector approaches lead III (the positive QRS complex in lead III), and distances itself from lead I (the negative QRS complex in lead I) (Figs. 1.19 and 1.20b).

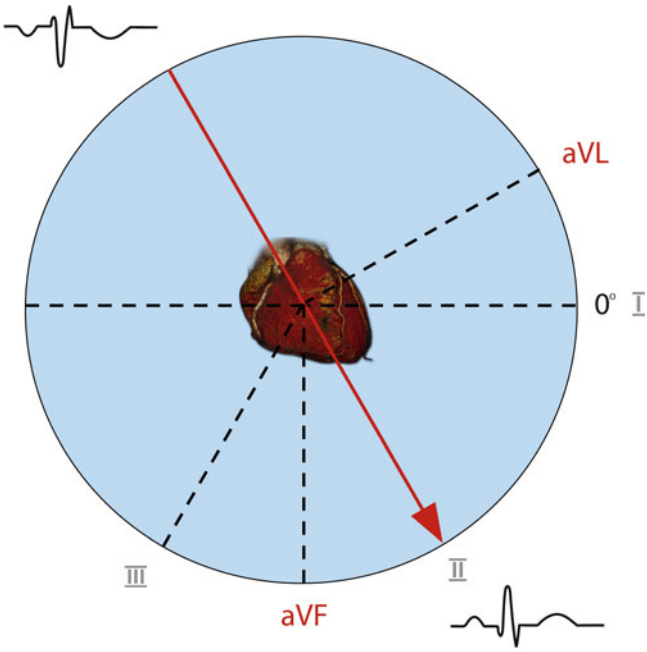

Fig. 1.18 The morphology of the ECG in leads aVR and II. Positive electrical impulses in the ECG directed toward the electrode (lead II) are registered as upward deflections, while the same impulses moving away from the electrode (aVR) are registered as downward deflections. In sinus rhythm when the depolarization is spread normally in the cardiac muscle the P-wave in lead II, the QRS complex, and the T-wave are positive

A detailed discussion of issues associated with arrhythmias and conduction problems are beyond the scope of this chapter. Hundreds of books, monographs, studies, and ECG articles have been dedicated to these topics; this is an old diagnostic procedure despite which a continuous progress is still being made (Fig. 1.21).

1.14 Conclusions

Applying digital methods to the ECG increases the resolution of the signal, thus enhancing its diagnostic capabilities. At the same time sophisticated methods also make it possible to apply algorithms that automatically interpret the ECG both in terms of morphology (the evaluation of multiple leads) and arrhythmias and conduction disorders (usually monitoring of a single lead is sufficient). Careful assessment of the ECG helps determine the mechanism and origin of the electrical impulse and propagation of electrical wave in the cardiac muscle and provides a wealth of useful information about the orientation of the heart, hypertrophy and